

COMMON ENVELOPE MECHANISMS: CONSTRAINTS FROM THE X-RAY LUMINOSITY FUNCTION OF HIGH MASS X-RAY BINARIES

ZHAO-YU ZUO^{1,3} AND XIANG-DONG LI^{2,3}

¹School of Science, Xi'an Jiaotong University, Xi'an 710049, China

²Department of Astronomy, Nanjing University, Nanjing 210093, China

³Key laboratory of Modern Astronomy and Astrophysics (Nanjing University), Ministry of Education, Nanjing 210093, China
zuozyu@mail.xjtu.edu.cn; lixd@nju.edu.cn

Draft version June 23, 2021

ABSTRACT

We use the measured X-ray luminosity function (XLF) of high-mass X-ray binaries (HMXBs) in nearby star-forming galaxies to constrain the common envelope (CE) mechanisms, which play a key role in governing the binary evolution. We find that the XLF can be reproduced quite closely under both CE mechanisms usually adopted, i.e., the α_{CE} formalism and the γ algorithm, with a reasonable range of parameters considered. Provided that the parameter combination is the same, the γ algorithm is likely to produce more HMXBs than the α_{CE} formalism, by a factor of up to ~ 10 . In the framework of the α_{CE} formalism, a high value of α_{CE} is required to fit the observed XLF, though it does not significantly affect the global number of the HMXB populations. We present the detailed components of the HMXB populations under the γ algorithm and compare them with those in Zuo et al. and observations. We suggest the distinct observational properties, as well as period distributions of HMXBs, may provide further clues to discriminate between these two types of CE mechanisms.

Subject headings: binaries: close - galaxies: evolution - galaxies: general - stars: evolution - X-rays: galaxies - X-ray: binaries - X-rays: stars

1. INTRODUCTION

The common envelope (CE) evolution is among the most important and least well-constrained processes in binary evolution. It is commonly thought to occur if the mass transfer is dynamically unstable. The result is that the accreting star spirals into the envelope of the donor star (see Iben & Livio 1993; Taam & Sandquist 2000; Webbink 2008; Taam & Ricker 2010; Ivanova et al. 2013, for reviews). The orbital energy and angular momentum of the accreting star are then transferred into the CE via an as of yet unknown mechanism. This may end with a stellar merger or, if the binary can survive, a binary with a much shorter orbital period. The CE evolution is critical in the formation of various kinds of compact binaries.

There have been extensive three dimensional hydrodynamical simulations (e.g., Rasio & Livio 1996; Sandquist et al. 1998, 2000; Fryxell et al. 2000; O'Shea et al. 2005; Fryer et al. 2006; Passy et al. 2012; Ricker & Taam 2012). However the physics of CE evolution still remains poorly understood, primarily due to a mix of various kinds of physical processes operating over a large range of timescales and length scales during the CE phase. Due to the difficulties in modeling the detailed CE evolution, population synthesis simulations commonly resort to simplified and parameterized descriptions to relate the post- and pre-CE orbital parameters (Tutukov & Yungleson 1979). One such parametrization dictates the CE phase in terms of a simple energy budget (known as the α_{CE} formalism, van den Heuvel 1976; Webbink 1984; Livio & Soker 1988; Iben & Livio 1993) and the other in terms of the angular momentum budget (named as the γ algorithm, Nelemans et al. 2000; Nelemans & Tout 2005). Both approaches have the power to account for

some specific classes of post-CE binaries (PCEBs), such as cataclysmic variables (CVs, King 1988), subdwarf B binaries (Morales-Rueda et al. 2003; Han et al. 2002, 2003), low-mass X-ray binaries (Charles & Coe 2006), and other compact objects thought to have suffered a merger, which are probably responsible for gamma-ray bursts (Fryer et al. 1999; Thöne et al. 2011) and Type Ia supernova (SNe Ia, Iben & Tutukov 1984; Belczynski et al. 2005; Ruiter et al. 2011; Meng et al. 2011; Meng & Yang 2012; Wang & Han 2012). There is an energetic debate over the two approaches in the literature.

High-mass X-ray binaries (HMXBs) are good examples of the effect of CE evolution. Luminous HMXBs usually have experienced CE evolution so that they have close orbits, which lead to a high wind-capture rate by the compact star. Tight orbits also help the binary survive the SN kick during the formation of the compact star. However, if the initial binary orbit is not large enough, CE evolution may lead to mergers, reducing the HMXB production. Thus, the populations and the specific characteristics (for example the orbital period distribution) of HMXBs can be used to probe the physical interactions during the CE phase.

The formation of HMXBs involves several evolutionary pathways (Van Bever & Vanbeveren 2000; Linden et al. 2010, see also Tauris & van den Heuvel 2006). Beginning with two relatively massive stars ($\gtrsim 10 M_{\odot}$), the more massive primary evolves and commences mass transfer to the secondary. The mass transfer can be either dynamically stable or unstable. In the latter case, CE evolution occurs that greatly shrinks the binary orbit. The resultant binary consists of the primary's core and the secondary. The primary's core then collapses to form a neutron star (NS) or black hole (BH). An HMXB ap-

pears when the compact star is able to accrete from the secondary by capture of the stellar wind or Roche lobe overflow (RLOF). Note that the secondary can be on the main-sequence (MS) or a (super)giant star. In some cases the second mass transfer may also lead to a CE phase, during which the envelope of the secondary is stripped, leaving a naked helium core. This leads to the formation of HMXBs with Wolf-Rayet companions.

HMXBs have some unique statistical characteristics (for catalogs, see Liu et al. 2005, 2006). One of the most striking features is that their X-ray luminosity function (XLF) follows a universal power law form over a broad X-ray luminosity range, from $\sim 10^{35}$ to $\sim 10^{40}$ ergs $^{-1}$. This was first discovered by Grimm, Gilfanov & Sunyaev (2003), and further confirmed recently by Mineo, Gilfanov & Sunyaev (2012, hereafter MGS12 for short). The XLF has been shown to follow a power law with a single slope of ~ 1.6 , without any significant feature near the critical Eddington luminosity of an NS or a stellar mass BH. Additionally, the collective luminosity of HMXB populations scales with the star formation rate (SFR) as $L_X(\text{ergs}^{-1}) \approx 2.6 \cdot 10^{39} \times \text{SFR}(M_\odot \text{ yr}^{-1})$.

In the present work, we apply the updated evolutionary population synthesis (EPS) techniques to model the XLF of HMXBs, taking into account both the α_{CE} algorithm and γ algorithm (with different choices of α_{CE} and γ , respectively), to describe the CE evolution. By comparing the observational sample with our theoretical expectations, we try to discriminate or constrain the effects of the two CE mechanisms.

This paper is organized as follows. In §2 we describe the population synthesis method and the input physics for X-ray binaries (XRBs) in our model. The calculated results and discussions are presented in §3. Our conclusions are in §4.

2. MODEL DESCRIPTION

We use the EPS code developed by Hurley et al. (2000, 2002) and recently updated by Zuo, Li & Gu (2014a) to calculate the expected number and the X-ray luminosity of HMXBs. In the present code, the model for compact object formation has been significantly revised by taking into account the formation of NSs through electron capture supernovae (ECS, Podsiadlowski et al. 2004) and the fallback process for both delayed and direct BH formation during core collapse (Fryer & Kalogera 2001). The prescriptions for the wind mass loss rates of massive stars (Vink et al. 2001, see also Belczynski et al. 2010) and the compact remnant masses (Fryer et al 2012, see also Belczynski et al. 2012) are adopted in the code. We also update the criteria for CE occurrence as described below.

2.1. The CE Phase

During the binary evolution, the mass ratio ($q = M_{\text{donor}}/M_{\text{accretor}}$) is a crucial factor determining the stability of mass transfer. If it is larger than a critical value, q_{crit} , the mass transfer is dynamically unstable and a CE phase follows (Paczynski 1976). The ratio q_{crit} varies with the evolutionary state of the donor star at the onset of RLOF and the mass loss mechanisms during the mass transfer (Hjellming & Webbink 1987; Webbink 1988; Podsiadlowski et al. 2002; Chen & Han 2008). In

this study, we adopt an updated q_{crit} for Hertzsprung gap donor star, recently calculated by Shao & Li (2014, also see the Appendix A in Zuo, Li & Gu 2014a for more details). If the primary is on the first giant branch (FGB) or the asymptotic giant branch (AGB), we use

$$q_{\text{crit}} = [1.67 - x + 2(\frac{M_{c1}}{M_1})^5]/2.13 \quad (1)$$

where M_{c1} is the core mass of the donor star, and $x = d \ln R_1 / d \ln M$ is the mass-radius exponent of the donor star. If the mass donor star is a naked helium giant, $q_{\text{crit}} = 0.784$ (see Hurley et al. 2002, for more details).

2.1.1. The α_{CE} formalism

In the energy budget approach, the CE evolution is parameterized in terms of the orbital energy and binding energy as $E_{\text{bind}} \equiv \alpha_{\text{CE}} \Delta E_{\text{orb}}$ (Webbink 1984, 2008), where the parameter α_{CE} describes the efficiency of converting the orbital energy (E_{orb}) into the kinetic energy, which is used to eject the envelope, and E_{bind} is the binding energy of the envelope. The CE evolution is governed by the following equation (Kiel & Hurley 2006):

$$\alpha_{\text{CE}} \left[\frac{GM_c M_2}{2a_f} - \frac{GM_c M_2}{2a_i} \right] = - \frac{GM_1 M_{\text{env}}}{R_{L1} \lambda}, \quad (2)$$

which yields the ratio of final (post-CE) and initial (pre-CE) orbital separations as

$$\frac{a_f}{a_i} = \frac{M_c M_2}{M_1} \frac{1}{M_c M_2 / M_1 + 2M_{\text{env}} / (\alpha_{\text{CE}} \lambda R_{L1})}, \quad (3)$$

where G is the gravitational constant, M_c the helium-core mass of the primary star (of mass M_1), M_2 the mass of the secondary star, R_{L1} the RL radius of the primary star, M_{env} the mass of the primary's envelope, a_i and a_f denote the initial and final orbital separations, respectively, and λ is a parameter related to the stellar mass-density distribution.

The λ value depends on the structure and evolution of the donor star. However, in previous studies, it was usually adopted as constant (~ 0.5) for simplicity (Hurley et al. 2002; Zuo et al. 2008). Here we calculate the values of λ from detailed stellar models including the contribution from the internal (and ionization) energies within the envelope (Zuo, Li & Gu 2014a, also see Xu & Li 2010 and Loveridge et al. 2011).

We consider three constant, global values of α_{CE} . For our basic model, we use $\alpha_{\text{CE}} = 0.5$ (Zuo, Li & Gu 2014a). We also consider two other extreme values of $\alpha_{\text{CE}} = 1.0$ and 0.1 since α_{CE} is expected to be no more than unity if we consider the internal energies in calculating E_{bind} . Different CE efficiencies for the first and second CE episodes are also examined to test its effect on the XLFs. Models with different values of α_{CE} are denoted as A01A01, A05A05, A10A10, A01A05, and A05A01, respectively, where the two digits following each letter correspond to the values of α_{CE} during the first and second CE episodes, respectively.

Alternatively, recent studies on WD binaries show that α_{CE} may be a function of binary parameters rather than constant (Politano & Weiler 2007; Zorotovic et al. 2000; De Marco et al. 2011; Davis et al. 2012), although the

final relationship has not yet been well developed. Following De Marco et al. (2011), we adopt

$$\alpha_{\text{CE}} = 0.05 \times q^{1.2}, \quad (4)$$

where q is the ratio of the donor's mass to the accretor's mass at the time of the CE interaction, and this model is denoted as AqAq.

2.1.2. The γ algorithm

In the angular momentum budget approach, the CE interaction is parameterized in terms of γ , the ratio of the fraction of angular momentum lost, and the fraction of mass loss:

$$\frac{\Delta J}{J} = \gamma \frac{M_{\text{env}}}{M_1 + M_2} \quad (5)$$

where ΔJ is the change of the total angular momentum (J) during the CE phase. Implicitly assuming the conservation of energy, the orbital separation after the CE is then given by

$$\frac{a_f}{a_i} = \left(\frac{M_1}{M_c}\right)^2 \left(\frac{M_c + M_2}{M_1 + M_2}\right) \left[1 - \gamma \left(\frac{M_{\text{env}}}{M_1 + M_2}\right)\right]^2 \quad (6)$$

This description was first suggested by Nelemans et al. (2000) in their investigation of the formation of double WD binaries. They found that when the energy approach is applied to describe the first CE phase, a negative value of α_{CE} is required, which is clearly unphysical. Among the possible solutions leading to the known close double WDs, Nelemans & Tout (2005) found that $0.5 < \gamma < 3$ for the first (putative) CE phase, and $1 < \gamma < 4$ for the second CE phase. They noted that a value of γ between 1.5 and 1.75 can account for all known observed PCEBs, including double WDs, pre-CVs, and sdB plus MS binaries.

For the γ algorithm, we consider several constant, global values of γ from 1.7 to 1.0, as well as different γ values for the first and second CE episodes in our calculation. These models are denoted as G17G17, G15G15, G13G13, G10G10, G10G17 and G17G10 where the two digits following each letter correspond to the values of γ during the first and second CE episodes, respectively.

In the study, we first compare the two mechanisms under the same assumptions, as described below. The parameter combination is kept the same as in Zuo, Li & Gu (2014a), where the best-fit model in the α_{CE} formalism is achieved. In this case, only values of γ and α_{CE} are changed to see their effects on the XLF. Then we manage to determine the best-fit model in the γ algorithm by varying all the key parameters, and see their effects on the XLF (see Table 1). Finally, the two mechanisms are compared under each best-fit model (i.e., model A05A05 vs. model M1).

2.2. Input Parameters

We follow the evolution of a large number of binary systems, initially consisting of two zero-age MS stars. As HMXBs in the MGS12 samples reside in nearby star-forming galaxies, we adopt a constant SFR for 50 Myr and a fixed subsolar metallicity ($0.5 Z_{\odot}$, where $Z_{\odot} = 0.02$) accordingly (see Zuo, Li & Gu 2014a, for details). Since the observed average XLF has already been normalized, we choose a Salpeter initial mass function (IMF)

Table 1

Parameters adopted for each model under the γ algorithm. Here q_0 is the initial mass ratio, IMF is the initial mass function, f binary fraction, $\eta_{\text{Edd,BH}}$ - the factor of super-Eddington accretion rate allowed for BH XRBs, σ_{kick} is the dispersion of kick velocity, $\eta_{\text{bol,BH(NS)}}$ is the bolometric correction factor for BH(NS) XRBs, STD is the standard stellar winds while WEAK represents the standard wind mass loss rate reduced to 50%, MT87 represents the IMF of Matteucci & Tornambè (1987). In the best-fit model of γ algorithm (M1), the parameters are as follows: SFH=50 Myr, $\alpha = 0$, $\eta_{\text{Edd,BH}}=20$, $f = 0.5$, $\sigma_{\text{kick}} = 110 \text{ km s}^{-1}$, $\eta_{\text{bol,BH}}=0.2$, $\eta_{\text{bol,NS}}=0.1$ and Salpeter IMF.

Model	$P(q_0)$	IMF	f	$\eta_{\text{Edd,BH}}$	σ_{kick}	winds
M1	$\propto q_0^0$	Salpeter	0.5	20	110	STD
M2	$\propto q_0^0$	Salpeter	0.5	20	110	WEAK
M3	$\propto q_0^0$	Salpeter	0.8	20	110	STD
M4	$\propto q_0^0$	Salpeter	0.5	100	110	STD
M5	$\propto q_0^0$	Salpeter	0.5	20	110	STD
M6	$\propto q_0^0$	MT87	0.5	20	110	STD
M7	$\propto q_0^0$	Salpeter	0.5	20	190	STD
M8	$\propto q_0^0$	Salpeter	0.5	20	265	STD

and set the mass range as $0.1 - 100 M_{\odot}$ for the normalization in order to be in parallel with MGS12¹. We evolve 10^6 primordial systems² and set up the same grid of initial parameters (primary mass, secondary mass and orbital separation) as in Hurley et al. (2002).

For the initial secondary's mass (M_2), a power law distribution of $P(q_0) \propto q_0^{\alpha}$ is assumed, where $q_0 \equiv M_2/M_1$. In our basic model, a flat distribution is assumed, i.e., $\alpha = 0$. We adopt a logarithmically flat distribution of initial orbital separations $\ln a$ (Hurley et al. 2002).

We assume a binary fraction $f = 0.5$ and that all binaries are initially in a circular orbit. For the SN kicks imparted on an NS, we assume a Maxwellian distribution with $\sigma_{\text{kick}} = 110 \text{ km s}^{-1}$ (Zuo, Li & Gu 2014b). For compact objects formed with partial mass fallback, the natal kicks are decreased by a factor of $(1-f_b)$ where f_b is the fraction of the stellar envelope that falls back after the SN explosion.

2.3. X-ray luminosity and source type

We adopt the same procedures to compute the $0.5 - 8$ keV X-ray luminosity for MS/super-giant (SG) HMXBs and Be-XRBs as in Zuo, Li & Gu (2014a). For wind accretion, we use the classical Bondi & Hoyle (1944) formula to calculate the mass transfer rate to the compact star. In the case of RLOF, we discriminate transient and persistent sources using the criteria in Lasota (2001, i.e., Eq. 36 therein) for MS and red giant (RG) donor. The corresponding X-ray luminosity is calculated as follows:

$$L_{\text{X},0.5-8\text{keV}} = \begin{cases} \eta_{\text{bol}} \eta_{\text{out}} L_{\text{Edd}} & \text{transients in outbursts} \\ \eta_{\text{bol}} \min(L_{\text{bol}}, \eta_{\text{Edd}} L_{\text{Edd}}) & \text{persistent systems,} \end{cases} \quad (7)$$

where η_{bol} is the bolometric correction factor converting the bolometric luminosity (L_{bol}) to the $0.5 - 8$ keV X-ray luminosity, ranging between ~ 0.1 and ~ 0.8

¹ We have improperly chosen an IMF of Kroupa (2001) and set the mass range as $5.0 M_{\odot} - +\infty$ for the normalization in Zuo, Li & Gu (2014a). The predicted HMXBs were overestimated by a factor of ~ 3 , but the results and basic conclusions of the paper remain largely unchanged (see Zuo, Li & Gu 2014b, for details).

² We also change the number of the binary systems by a factor of eight, and find no significant difference in the final results.

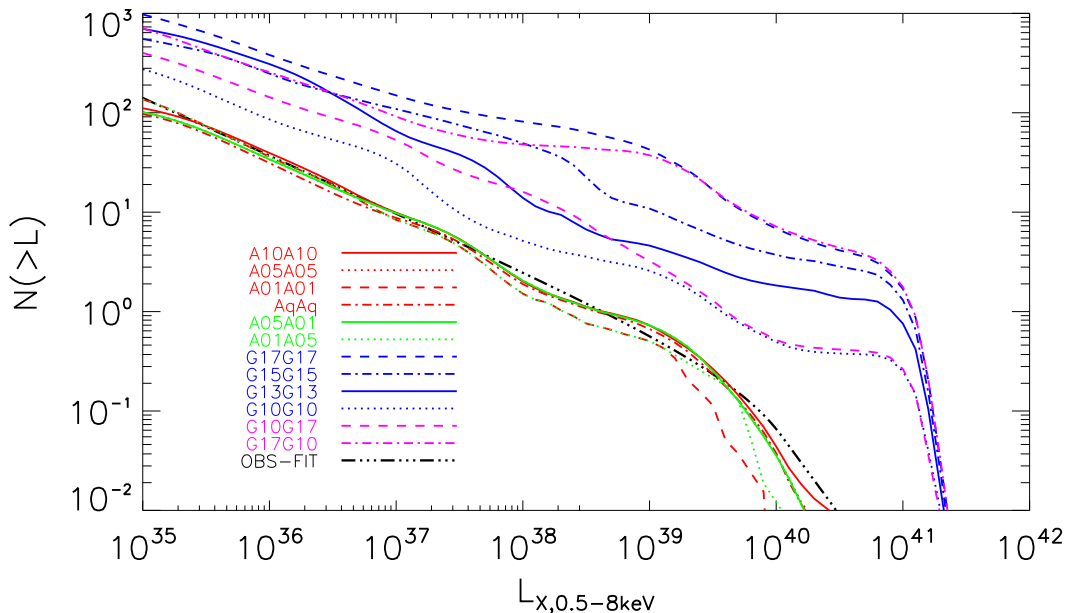


Figure 1. Simulated XLFs of different models on the treatment of the CE phase. The thick triple dot-dashed line represents the observed average XLF (labeled as ‘OBS-FIT’) derived by MGS12 using the data of 29 nearby star-forming galaxies.

(Belczynski et al. 2008); $L_{\text{bol}} \simeq 0.1 \dot{M}_{\text{acc}} c^2$ where \dot{M}_{acc} is the average mass accretion rate and c is the velocity of light. The critical Eddington luminosity $L_{\text{Edd}} \simeq 4\pi G M m_p c / \sigma_T = 1.3 \times 10^{38} m \text{ erg s}^{-1}$ (where σ_T is the Thomson cross section, m_p the proton mass, and m the accretor mass in the units of solar mass). We introduce the ‘Begelman’ factor η_{Edd} to allow super-Eddington luminosities. We fix $\eta_{\text{Edd,NS}} = 5$ for NS XRBs (Zuo, Li & Gu 2014a); for BH XRBs, $\eta_{\text{Edd,BH}}$ is set as a free parameter in the study. For transient sources, the outburst luminosity is taken as a fraction (η_{out}) of the critical Eddington luminosity. We take $\eta_{\text{out}} = 0.1$ and 1 for NS(BH) transients with orbital period P_{orb} less and longer than 1 day (10 hr), respectively (Chen et al. 1997; Garcia et al. 2003; Belczynski et al. 2008).

For Be-XRBs we employ a phenomenological definition as in Zuo, Li & Gu (2014a, also see Belczynski & Ziolkowski, 2009). Technically, we randomly select 25% ($f_{\text{Be}} = 0.25$, Slettebak 1988; Ziolkowski 2002; McSwain & Gies 2005) of NS binaries hosting a ($3.0 M_{\odot} - 20.0 M_{\odot}$) B/O star to be Be-XRBs, and estimate their numbers. The X-ray luminosity of a Be-XRB is calculated using the empirical relation (Eq. 11) in Dai et al. (2006), which is based on the data compiled by Raguzova & Popov (2005). Considering the duration of type I outbursts in Be-XRBs ($\sim 0.2 - 0.3 P_{\text{orb}}$, Reig 2011), we adopt an upper value of the duty cycle $DC_{\text{max}} = 0.3$ to calculate the source numbers.

3. RESULTS

We first compare the results in the α_{CE} formalism and γ algorithm under the same input parameters: SFH=50 Myr, $\alpha = 0$, $\eta_{\text{Edd,BH}}=100$, $f = 0.5$, $\sigma_{\text{kick}} = 110 \text{ km s}^{-1}$, $\eta_{\text{bol,BH}}=0.6$, $\eta_{\text{bol,NS}}=0.3$ and Salpeter IMF (Zuo, Li & Gu 2014a). For each CE episode, models are designed by changing only one parameter each time to test its effect. Figure 1 compares the simulated XLFs

with different treatments of the CE phase. Clearly, under the same parameter combination the γ algorithm can produce more (up to one order of magnitude) HMXBs than the α_{CE} formalism. In the framework of the α_{CE} formalism, though all models can fit the observed XLF quite closely in most of the luminosity range (i.e., $10^{35} - \sim 10^{39} \text{ erg s}^{-1}$), a high value of α_{CE} seems more preferable. This is mainly due to the sparseness of short period RLOF HMXBs in the case of smaller α_{CE} (compare with the right panel of Figure 1 in Zuo, Li & Gu 2014a), the progenitors of which coalesce during the binary evolution, especially in the first CE phase (see models A05A01 and A01A01). In the case of γ algorithm, the normalization of the simulated XLFs is rather sensitive to the value of γ , especially in the first CE phase (see models G10G17 and G17G17 or models G10G10 and G17G10). Smaller values of γ give a better fit to the observed XLF, not only in the normalization, but also in the overall shape. Considering that many parameters may considerably influence the XLF (Zuo, Li & Gu 2014a), further thorough parameter studies are needed to determine the best-fit model in the γ algorithm.

The key parameters we vary include: the binary fraction f , the super-Eddington factor η_{Edd} , the bolometric correction factor η_{bol} , the mass ratio, the IMF, the natal kick distribution, the wind mass loss rates and the value of γ . Some parameters affect only the normalization, such as f and η_{bol} ; some affect only the shape, for example, η_{Edd} ; while others affect both. We perform a suite of EPS models and find that the best-fit model in the γ algorithm can be achieved when parameters are adopted as follows: SFH=50 Myr, $\alpha = 0$, $\eta_{\text{Edd,BH}}=20$, $f = 0.5$, $\sigma_{\text{kick}} = 110 \text{ km s}^{-1}$, $\eta_{\text{bol,BH}}=0.2$, $\eta_{\text{bol,NS}}=0.1$, Salpeter IMF and $\gamma = 1.0$ (i.e., model M1). We also examine other values of γ , and find that the results are not better than in the case of $\gamma = 1.0$ (especially when

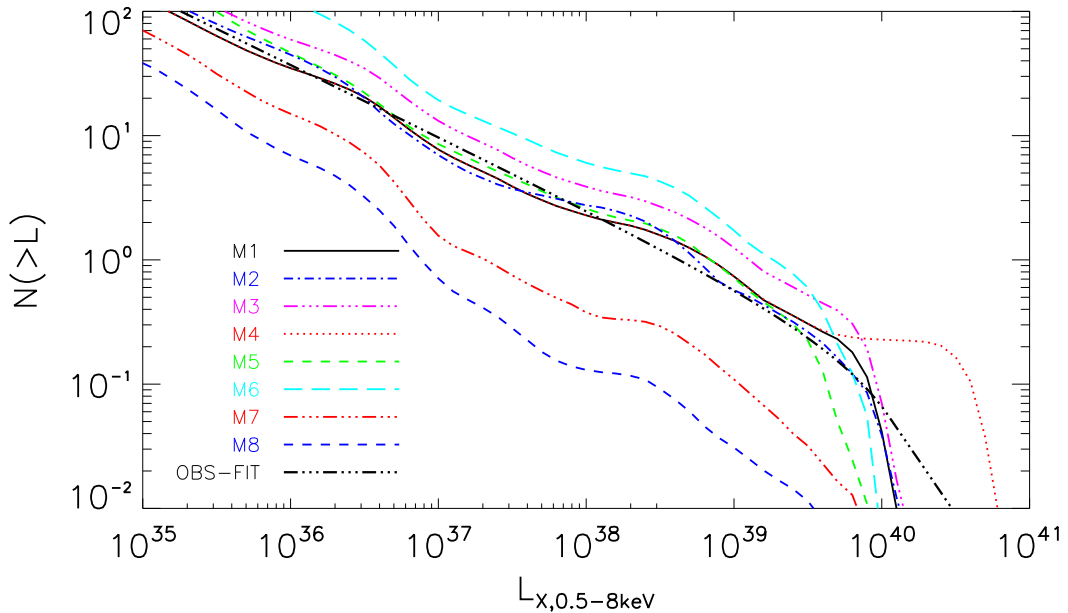


Figure 2. Comparisons of the simulated (models M1-M8, all under the γ -algorithm) and observed average (labeled as ‘OBS-FIT’, thick triple dot-dashed line) XLFs. Compared to the basic model M1 (solid line), in M2 (dash-dotted line), the standard wind mass loss rate is reduced by a factor of 2. In M3 (triple dot-dashed line), the binary fraction f is set as 0.8. In M4 (dotted line), the factor for super-Eddington accretion rate for BHs is set as 100 for comparison. We take an atypical distributions of mass ratio in M5 (short-dashed line) and a flatter IMF in M6 (long-dashed line), respectively. In models M7 and M8, the dispersion of kick velocity is increased to $\sigma_{\text{kick}} = 190 \text{ km s}^{-1}$ (triple dot-dashed line) and $\sigma_{\text{kick}} = 265 \text{ km s}^{-1}$ (short-dashed line), respectively.

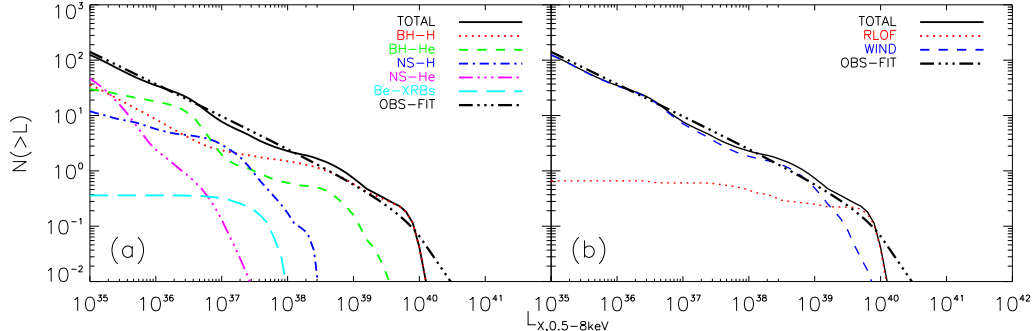


Figure 3. Detailed components of the simulated XLF (panel a) and the accretion modes of simulated XRBs (panel b) in model M1. Panel (a): The solid, dotted, short-dashed, dash-dotted, triple dot-dashed, long-dashed lines represent ALL-XRBs, BH-H, BH-He, NS-H, NS-He MS/SGXRBs and Be-XRBs, respectively. Panel (b): The solid, dotted, dashed lines represent ALL-XRBs, RLOF-fed XRBs and wind-fed XRBs, respectively. The thick triple dot-dashed line represents the derived average XLF (labeled as ‘OBS-FIT’) by MGS12 using the data of 29 nearby star-forming galaxies.

$\gamma \gtrsim 1.5$). In order to show the dependences of the XLF on the parameters, we also change these parameters one by one. The details are listed in Table 1.

Figure 2 clearly shows that the parameters act in different ways. Several parameters have only minor effects, i.e., the wind mass loss rate (model M2) and the initial mass ratio distribution of the secondary star (model M5). Some (e.g. models M3 and M6) mainly increase the number of HMXB populations. An increase of the binary fraction (model M3) gives more XRBs, hence an overall shift of the XLF. A flatter IMF (model M6) reflects more massive stars, hence more compact objects that may result in XRBs. An increase of the dispersion velocity σ_{kick} (models M7 and M8) means that the natal kicks of higher magnitude are chosen more frequently from the

Maxwellian distribution, hence more disruptions of binaries during the SN explosions. This decreases the number of potential HMXBs, and meanwhile changes the shape of the XLF. We note the large uncertainties in σ_{kick} , f , and η_{bol} make it difficult to tightly constrain the value of γ . The apparent luminosity ‘knee’ of XLFs is weakened if we restrict the super-Eddington factor to 20 (compare model M4 with others), implying that the maximum super-Eddington luminosity allowed is likely ~ 20 in the case of γ algorithm. To sum up, in the framework of the γ algorithm, the observed XLF can also be reconstructed within the reasonable range of the parameters adopted.

In order to explore the nature of HMXBs in the case of γ algorithm, we also examine the detailed observational properties (i.e., orbital period, the current mass

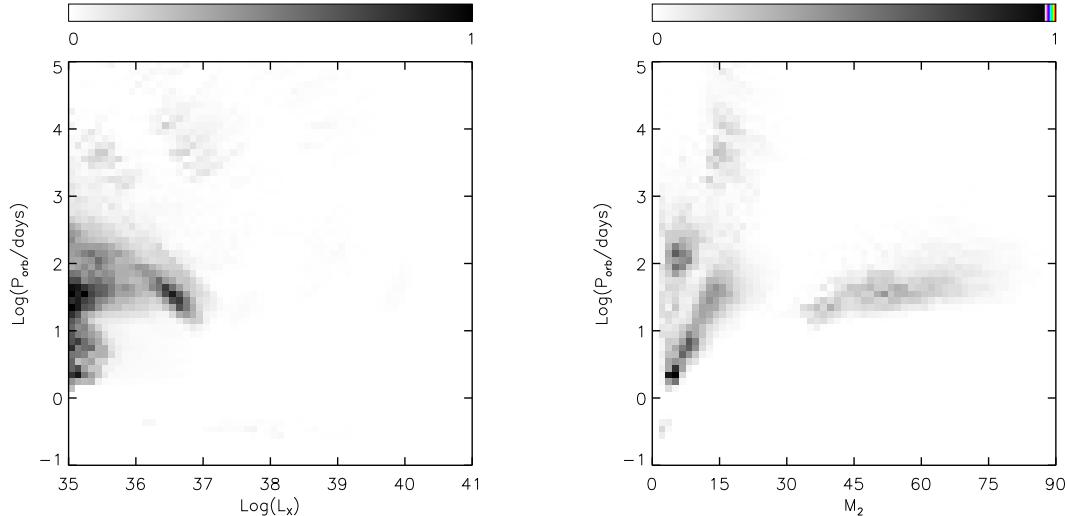


Figure 4. Current orbital period $P_{\text{orb}} - L_X$ (left) and $P_{\text{orb}} - M_2$ (right) distributions in model M1.

M_2 of the donor star, etc.) of the simulated HMXBs, and compare them with those in Zuo, Li & Gu (2014a, i.e. α_{CE} formalism) and observations. Shown in Figure 3 are the detailed components of the simulated XLF (left) and the accretion modes in XRBs (right) and in Figure 4 are the $P_{\text{orb}} - L_X$ (left) and $P_{\text{orb}} - M_2$ (right) distributions in model M1. It is clear that under the γ algorithm BH-He XRBs dominate in the low luminosity range (i.e., $L_X < \sim 10^{37} \text{ erg s}^{-1}$) of the XLF while this is not the case in the α_{CE} formalism, where BH-MS XRBs instead dominate (Zuo, Li & Gu 2014a). Unfortunately, due to the limited instrument capabilities available, most of the extragalactic X-ray sources remain unresolved. We still do not clearly know their nature (for example, the spectral type of the donor star and the type of the compact star), especially the sources in low luminosities. We suggest further check with higher-precision observations is still needed in the future. The orbital period distribution is also distinct from that in Zuo, Li & Gu (2014a), with a much larger population of relatively short period (less than several tens of days) systems. This is more clearly revealed in Figure 5 for the normalized orbital period P_{orb} distribution in models A05A05 (left) and M1 (right). We can see that short period HMXB population keeps growing under the γ algorithm, while most HMXBs under the α_{CE} formalism are produced within the first 20 Myrs. These distinct observational properties of HMXBs, as well as different period distributions may provide further clues to discriminate between the two models.

We note the discrepancy in the BH-He HMXB population between models is solely a result of different treatments on CE, in which the γ algorithm predicts a survival, while the α_{CE} formalism predicts a merger instead. The progenitors of BH-He HMXBs always have the following features. First, the primary stars are very massive, $\sim 30 - 80 M_{\odot}$, so they can form BHs in a mild (with low/no kicks) way, which will not disrupt the system. Second, the companion stars are relatively less massive, i.e., $\sim 10 - 35 M_{\odot}$. The orbits of the binaries are not too wide, of the order of tens to hundreds of R_{\odot} .

These conditions guarantee that the primary can overflow its RL rapidly and transfer mass in a dynamically stable way (because the mass ratio is not too extreme³). After that, the primary evolves to a BH, and the rejuvenated secondary star expands and fills its RL. However, due to the large mass ratio, the mass transfer this time is unstable, and a CE is triggered. The α_{CE} formalism always leads to binary mergers due to the huge amount of binding energy in the giant envelope. In the case of γ algorithm, the orbital evolution is determined by the mass ratio $q = M_{\text{donor}}/M_{\text{accretor}}$ and the core mass fraction $\mu = M_c/M_{\text{donor}}$. From Eq. 6 in Nelemans & Tout (2005), it is easy to deduce that the binary orbit not only shrinks (but still different from that in the α_{CE} formalism), but also expands (see also Figure 3 therein). This expansion of the orbit not only avoids binary mergers, but also delays the XRB formation significantly. This is also why, under the same assumptions the γ algorithm can produce more HMXBs than the α_{CE} formalism and the HMXBs can keep emerging after 20 Myr in the case of the γ algorithm.

To illustrate the formation and evolution of a typical BH-He HMXB, we present one example evolutionary sequence for M_1 , M_2 , P_{orb} , and L_X under the γ algorithm in Figure 6. We consider a primordial binary system in a $\sim 91.44 R_{\odot}$ circular orbit. The initial stellar masses are 35.493 and $12.532 M_{\odot}$ for the primary and secondary, respectively. The primary evolves first, and fills its RL on the HG (at 5.5483 Myr). The mass transfer proceeds rapidly as it evolves across the HG until the end of CHeB, at which point (5.5598 Myr) it becomes an $11.069 M_{\odot}$ HeMS star with a $34.451 M_{\odot}$ (rejuvenated) MS star in a $109.626 R_{\odot}$ orbit. Shortly after that, the naked helium star evolves across the HeHG and collapses at 6.2418 Myr, leaving a $7.617 M_{\odot}$ BH with an MS companion in a $167.93 R_{\odot}$ orbit. Subsequently, the MS star evolves to expand and fills its RL on the HG, and then the binary

³ If the mass ratio is extreme, a CE is triggered, followed by a second CE between the newly formed BH and an expanding giant, instead resulting in much tighter BH-HeMS XRBs instead. However, their population is relatively minor in this case.

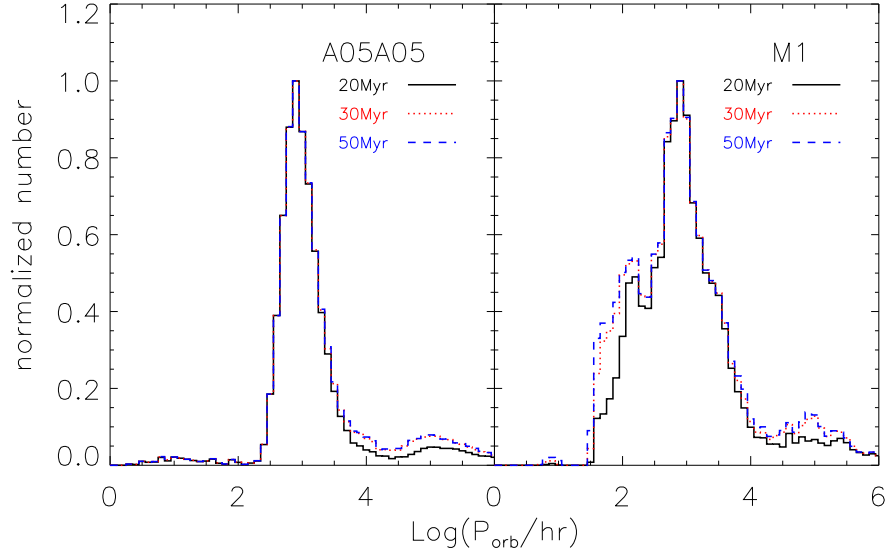


Figure 5. Orbital period P_{orb} distribution in models A05A05 (left) and M1 (right), respectively. The number is normalized for comparison. The solid, dotted, and dashed lines represent SFH of 20, 30 and 50 Myr, respectively.

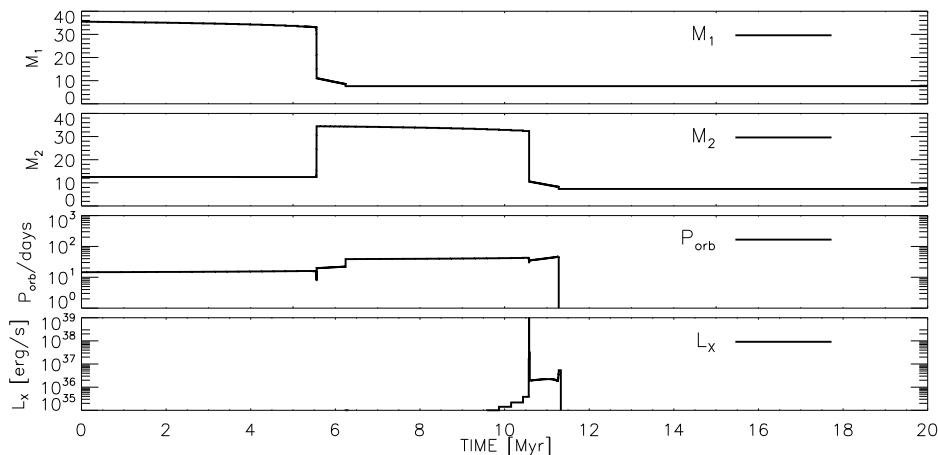


Figure 6. Evolution of M_1 , M_2 , P_{orb} , and L_X for an example of short orbital period BH-He HMXBs under the γ algorithm (model M1).

enters into the CE stage (10.5754 Myr). At this time, the mass ratio is $q \sim 4.3$ and the core mass fraction $\mu \sim 0.3$, and the orbit shrinks slightly from $134.38 R_{\odot}$ to $118.55 R_{\odot}$, as calculated from Eq. 6 in Nelemans & Tout (2005). At the end of the CE, the envelope of the giant star is expelled, leaving a $10.58 M_{\odot}$ HeMS star. The stellar wind from the HeMS star is then accreted by the BH, resulting in a BH-HeMS XRB. At last, the HeMS evolves to explode as an SN (11.28 Myr), which results in a $7.348 M_{\odot}$ BH and disrupts the binary system.

Our findings are generally consistent with other previous studies concerning the CE evolution. For example, in the case of the α_{CE} formalism, a high value of α_{CE} is required to account for the observed WDMS PCEBs ($\alpha_{\text{CE}} \gtrsim 0.1$, Davis et al. 2010), the shape of the delay-time distribution and the birth rate of SNe Ia for the double-degenerate systems (Meng & Yang 2012), and the displacements of HMXBs ($\alpha_{\text{CE}} \sim 0.8 - 1.0$, Zuo & Li 2014c), while a lower value of α_{CE} may be excluded (Meng & Yang 2012; Zuo & Li 2014c). An exception is from Fragos et al. (2013) where a low value

of $\alpha_{\text{CE}} \sim 0.1$ is preferred, most likely due to the oversimplified treatments for the binding energy parameter, where λ is adopted as one overall, while this is not the case for massive stars ($\lambda \sim 0.1$, Xu & Li 2010). It is interesting to note that to create double WDs, the standard α_{CE} formalism is also possible if the first mass transfer between an RG and an MS star can be stable and non-conservative. This leads to a modest widening of the orbit, with an effect similar to the γ algorithm (Woods et al. 2012). In the framework of the α_{CE} formalism, our simulations are also comparable to previous studies concerning HMXB populations (Portegies Zwart & Verbunt 1996; Terman, Taam & Savage 1998; Linden et al. 2010). The major formation pathways of HMXBs in Zuo, Li & Gu (2014a) are consistent with the results obtained by Linden et al. (2010). The predicted observational properties of HMXBs (such as the orbital period distributions) are also similar. The number of HMXBs is also found to be not very sensitive to the value of α_{CE} . However, it seems that neither the α_{CE} formalism nor the γ

algorithm can account for all the specific classes of observed PCEBs (Meng et al. 2011; Meng & Yang 2012). Moreover, even within the framework of the α_{CE} formalism, different studies often give controversial results on the possible range of α_{CE} and its dependence on other parameters (see Zorotovic et al. 2000; De Marco et al. 2011; ?; Toonen & Nelemans 2013, also Ivanova et al. 2013 and references therein). Our work suggests that in the case of HMXBs, both the α_{CE} formalism and the γ algorithm are possible to reproduce the observed XLF. In the framework of α_{CE} formalism, a high value of α_{CE} is needed, although a constant value is not required. We also show the distinct observational properties, such as the period distribution of HMXBs, that may serve as possible keys to understanding the CE evolution and to discriminate between different CE models.

4. SUMMARY

We have used an EPS code to model the XLF of HMXBs with a range of theoretical models describing the CE phase. Our study shows that the observed XLF can be reproduced quite closely under both CE mechanisms. Provided that the same parameter combination is chosen, the γ algorithm seems to produce more HMXBs than the α_{CE} formalism, by a factor of up to ~ 10 . Additionally, in the framework of the α_{CE} formalism, a high value of α_{CE} around $\sim 0.5 - 1.0$ better fits the observed XLF. We present the detailed properties of HMXB populations under the γ algorithm, and find that the simulated HMXBs have a much larger population of short period (less than about several tens of days) BH-He systems than in the α_{CE} formalism, which may serve as clues to discriminate between the two kinds of models. Our work motivates further high-resolution X-ray and optical observations of HMXB populations in nearby star-forming galaxies.

We thank the anonymous referee for helpful suggestions that enabled us to improve the manuscript. This work was supported by the National Natural Science Foundation (under grant numbers 11103014, 11003005, 11133001, 11333004, and 10873008), the Research Fund for the Doctoral Program of Higher Education of China (under grant number 20110201120034), the National Basic Research Program of China (973 Program 2009CB824800), the Strategic Priority Research Program of CAS under grant No. XDB09010200, and the Fundamental Research Funds for the Central Universities.

REFERENCES

- Belczynski K., Bulik T., Ruiter A. J., 2005, *ApJ*, 629, 915
 Belczynski K., Bulik T., Fryer C., Ruiter A., Valsecchi F., Vink J. S., Hurley J. R., 2010, *ApJ*, 714, 1217
 Belczynski K., Kalogera V., Rasio F. A., Taam R. E., Zezas A., Bulik T., Maccarone T. J., Ivanova N., 2008, *ApJS*, 174, 223
 Belczynski K., Wiktorowicz G., Fryer C. L., Holz D. E., Kalogera V., 2012, *ApJ*, 757, 91
 Belczynski K., Ziolkowski J., 2009, *ApJ*, 707, 870
 Bondi H., Hoyle F., 1944, *MNRAS*, 104, 273
 Charles, P. A., & Coe, M. J. 2006, in *Compact Stellar X-ray Sources*, ed. W. H. G. Lewin & M. van der Klis (Cambridge: Cambridge Univ. Press), 215
 Chen X., Han Z., 2008, *MNRAS*, 387, 1416
 Chen W., Shrader C. R., Livio M., 1997, *ApJ*, 491, 312
 Dai H. L., Liu X. W., Li X. D., 2006, *ApJ*, 653, 1410
 Davis P. J., Kolb U., Willems B., 2010, *MNRAS*, 403, 179
 Davis P. J., Kolb U., Knigge C., 2012, *MNRAS*, 419, 287
 De Marco O., Passy J., Moe M., Herwig F., Mac Low M., Paxton B., 2011, *MNRAS*, 411, 2277
 Fragos T., Lehmer B., Tremmel M., Tzanavaris P., Basu-Zych A., Belczynski K., Hornschemeier A., Jenkins L., Kalogera V., Ptak A., Zezas, A., 2013, *ApJ*, 764, 41
 Fryer C. L., Belczynski K., Wiktorowicz G., Dominik M., Kalogera V., Holz D. E., 2012, *ApJ*, 749, 91
 Fryer C.L., Kalogera V., 2001, *ApJ*, 554, 548
 Fryer C. L., Rockefeller G., Warren M. S., 2006, *ApJ*, 643, 292
 Fryxell B., Olson K., Ricker P., Timmes F. X., Zingale M., Lamb D. Q., MacNeice P., Rosner R., Truran J. W., Tufo H., 2000, *ApJS*, 131, 273
 Fryer C. L., Woosley S. E., Hartmann D. H., 1999, *ApJ*, 526, 152
 Garcia M. R., Miller J. M., McClintock J. E., King A. R., Orosz J., 2003, *ApJ*, 591, 388
 Grimm H.-J., Gilfanov M., Sunyaev R., 2003, *MNRAS*, 339, 793
 Han Z., Podsiadlowski P., Maxted P. F. L., Marsh T. R., 2003, *MNRAS*, 341, 669
 Han Z., Podsiadlowski P., Maxted P. F. L., Marsh T. R., Ivanova N., 2002, *MNRAS*, 336, 449
 Hjellming M.S., Webbink R.F., 1987, *ApJ*, 318, 794
 Hurley J. R., Pols O. R., Tout C. A., 2000, *MNRAS*, 315, 543
 Hurley J. R., Tout C. A., Pols O. R., 2002, *MNRAS*, 329, 897
 Iben I. Jr, Livio M., 1993, *PASP*, 105, 1373
 Iben Jr., I. Tutukov A. V., 1984, *ApJ Supp*, 54, 335
 Ivanova, N. et al., 2013, *A&A Review*, 21, 591
 Kiel P.D., Hurley J.R., 2006, *MNRAS*, 369, 1152
 King A. R., 1988, *QJRAS*, 29, 1
 Kroupa P., 2001, *MNRAS*, 322, 231
 Lasota J. P., 2001, *New Astronomy Reviews*, 45, 449
 Linden T., kalogera V., Sepinsky J. F., Prestwich A., Zezas A., Gallagher J. S., 2010, *ApJ*, 725, 1984
 Liu Q. Z., van Paradijs J., van den Heuvel E. P. J., 2005, *A&A*, 442, 1135
 Liu Q. Z., van Paradijs J., van den Heuvel E. P. J., 2006, *A&A*, 455, 1165
 Livio M., Soker N., 1988, *ApJ*, 329, 764
 Loveridge A. J., van der Sluys M. V., Kalogera V., *ApJ*, 2011, 743, 49
 Matteucci F., Tornambè A., 1987, *A&A*, 185, 51
 McSwain M. V., Gies D. R., 2005, *ApJS*, 161, 118
 Meng X., Chen W., Yang W., Li Z., 2011, *A&A*, 525, A129
 Meng X., & Yang W., 2012, *A&A*, 543, A137
 Mineo S., Gilfanov M., Sunyaev R., 2012, *MNRAS*, 419, 2095 (MGS12)
 Morales-Rueda L., Maxted P. F. L., Marsh T. R., North R. C., Heber U., 2003, *MNRAS*, 338, 752
 Nelemans G. & Tout C. A., 2005, *MNRAS*, 356, 753
 Nelemans G., Verbunt F., Yungelson L. R., Portegies Zwart S. F., 2000, *A&A*, 360, 1011
 O'Shea B. W., Nagamine K., Springel V., Hernquist L., Norman M. L., 2005, *ApJ Supp*, 160, 1
 Paczyński P., 1976, in Eggleton P., Mitton S., Whelan J., eds, *Proc. IAU Symp. 73, Structure and Evolution of Close Binary Systems*, p. 75
 Passy J.-C., De Marco O., Fryer C. L., Herwig F., Diehl S., Oishi J. S., Mac Low M.-M., Bryan G. L., Rockefeller G., 2012, *ApJ*, 744, 52
 Podsiadlowski P., Langer N., Poelarends A. J. T., Rappaport S., Heger A., Pfahl E., 2004, *ApJ*, 612, 1044
 Podsiadlowski P., Rappaport S., Pfahl E. D., 2002, *ApJ*, 565, 1107
 Politano M., Weiler M., 2007, *ApJ*, 665, 663
 Portegies Zwart S. F., Verbunt F., 1996, *A&A*, 309, 179
 Raguzova N. V., Popov S. B., 2005, *Astron. Astrophys. Trans.*, 24, 151
 Rasio F., Livio M., 1996, *ApJ*, 471, 366
 Reig P., 2011, *Ap&SS*, 332, 1
 Ricker, P. M. & Taam, R. E., 2012, *ApJ*, 746, 74
 Ruiter A. J., Belczynski K., Sim S. A., Hillebrandt W., Fryer C. L., Fink M., Kromer M., 2011, *MNRAS*, 417, 408
 Sandquist E. L., Taam R. E., Burkert A., 2000, *ApJ*, 533, 984
 Sandquist E. L., Taam R. E., Chen X., Bodenheimer P., Burkert A., 1998, *ApJ*, 500, 909
 Shao Y., Li X. D., 2014, in preparation
 Slettebak A., 1988, *PASP*, 100, 770

- Taam R. E. Ricker P. M., 2010, *New Astronomy Reviews*, 54, 65
- Taam R., Sandquist E., 2000, *ARA&A*, 38,113
- Tauris T. M., van den Heuvel E. P. J., 2006, in Lewin W., van der Klis M., eds, *Compact Stellar X-ray Sources*. Cambridge Univ. Press, Cambridge, p. 623
- Terman J. L., Taam R. E., Savage C. O., 1998, *MNRAS*, 293, 113
- Thöne C. C., de Ugarte Postigo A., Fryer C. L., Page K. L., Gorosabel J., Aloy M. A., Perley D. A., Kouveliotou C., et al., 2011, *Nature*, 480, 72
- Toonen S., Nelemans G., 2013, *A&A*, 557, A87
- Tutukov, A., & Yungelson, L. 1979, in *IAU Symp. 83, Mass Loss and Evolution of O-Type Stars*, ed. P. S. Conti & C. W. H. De Loore (Dordrecht: Reidel), 401
- Van Bever, J., & Vanbeveren, D. 2000, *A&A*, 358, 462
- van den Heuvel E. P. J., 1976, in *IAU Symposium, Vol. 73, Structure and Evolution of Close Binary Systems*, ed. P. Eggleton, S. Mitton, & J. Whelan, 35
- Vink J. S., de Koter A., Lamers H. J. G. L. M., 2001, *A&A*, 369, 574
- Wang, B., Han, Z. 2012, *NewAR*, 56, 122
- Webbink R. F., 1984, *ApJ*, 277, 355
- Webbink, R. F. 2008, in *Short-Period Binary Stars: Observations, Analyses, and Results*, ed. E. F. Milone, D. A. Leahy, & D. W. Hobill (Astrophysics and Space Science Library, Vol. 352; Berlin: Springer), 233
- Webbink R. F., 2008, in *Astrophysics and Space Science Library, Vol. 352, "Short-Period Binary Stars: Observations, Analyses, and Results"*, ed. E. F. Milone, D. A. Leahy, & D. W. Hobill, 233
- Woods, T. E., Ivanova, N., van der Sluys, M. V., & Chaichenets, S. 2012, *ApJ*, 744, 12
- Xu X. J., Li X. D., 2010, *ApJ*, 716, 114
- Ziolkowski J., 2002, *MmSAI*, 73, 1038
- Zorotovic M., Schreiber M. R., Gänsicke B. T., Nebot Gómez-Morán A., 2010, *A&A*, 520, 86
- Zuo Z. Y., Li X. D., Gu Q. S., 2014a, *MNRAS*, 437, 1187
- Zuo Z. Y., Li X. D., Gu Q. S., 2014b, *MNRAS*, 443, 1889
- Zuo Z. Y., Li X. D., Liu X. W., 2008, *MNRAS*, 387, 121
- Zuo Z. Y., Li X. D., 2014c, *MNRAS*, 442, 1980